AIAA 81-0744R

Plasma Propagation Simulation Near an Electrically Propelled Spacecraft

R.S. Robinson,* H.R. Kaufman,† and D.R. Winder‡
Colorado State University, Fort Collins, Colo.

A charge-exchange plasma environment is produced by an electrostatic ion thruster. It is important to understand the possible interaction of various spacecraft systems with this plasma. To this end, a detailed knowledge of the propagation of a charge-exchange plasma in the vincinity of a spacecraft is important. A model that describes the charge-exchange plasma and its propagation is described, along with a computer code based on this model. The geometry of an idealized spacecraft with an ion thruster is outlined, together with the assumptions used in modeling the ion beam. The distribution function describing charge-exchange ion production is also presented. The barometric equation is used to relate the variation in plasma potential to the variation in plasma density. Comparisons between the computer simulation and experimental data are presented. The model is in good qualitative and quantitative agreement with experimental plasma density and ion trajectory angle measurements. An analytical solution of a simple configuration is also used to verify the model.

Nomenclature

C = constant of proportionality for ion density calculations
d = distance between ion trajectories
e = electronic charge
F = force on an ion
J_b = beam current
j_b = beam current density
m_0 = propellant mass
$\dot{N}_{CE}$ = charge-exchange ion production rate
$\dot{N}_0$ = neutral loss rate
n_e = electron density
n_0 = neutral gas concentration
Q = charge-exchange cross section
q = charge
r = distance from beam axis
r_b = beam radius
T_e = electron temperature
T_0 = propellant temperature
t = time
V = local plasma potential
V_0 = reference plasma potential
v = ion velocity
v_{CE} = Bohm velocity
z = distance from thruster along the beam
$\delta(\vec{r})$ = Dirac delta function
θ = azimuth angle measured about thruster axis

Introduction

THE production of charge-exchange ions by electric thrusters and the interaction of a thruster with the other components of an electrically propelled spacecraft through the space surrounding a spacecraft have been studied for some time. The transport of electrons from the ion beam to a positive solar array was first treated by Knauer et al.[1] as an electron space charge flow problem. Measured electron currents, however, were found to be much higher than calculated by Knauer and the bulk of the difference was due to the presence of a charge-exchange plasma.

The production rate for the charge-exchange ions was first calculated by Staggs et al.[2] The capability of the charge-exchange plasma to transport electrons to other parts of the spacecraft was experimentally evaluated by Worlock et al.[3] Some detailed trajectories of charge-exchange ions have been examined by Komatsu et al.[4] An experimental study of the distribution of the charge-exchange plasma, particularly upstream of the ion beam direction, was conducted by Kaufman[5-7] and by Kaufman and Isaacson.[8] These experimental studies included work on a correlation of plasma properties in terms of the distance from the thruster and the angle relative to the beam direction.

Charge-Exchange Plasma Generation

Of the several categories of ions present in the efflux of an ion thruster,[2] only group IV or low-energy ions will be considered here because such ions can follow trajectories that depart substantially from straight lines. Two types of processes generating these charge-exchange ions can take place within the beam volume of an ion thruster. The dominant process takes place when fast beam ions accelerated from the thruster exchange single electrons with the much slower neutral propellant atoms that are also escaping as a gas flow through the accelerator system. This process results in the production of ions that initially have a thermal velocity corresponding only to the average wall temperature of the interior of the discharge chamber. Charge exchange of this kind between like atoms is termed resonance charge exchange and is typically characterized by a larger cross section at a given relative energy than nonresonance charge exchange between unlike atoms. The process of nonresonance charge exchange can take place between fast beam ions and sputtered efflux from the thruster such as Mo from the accelerator grid. Normally, nonresonance charge exchange processes can be neglected compared to resonance charge exchange. In some instances there might be concern about the deposition of metallic layers on delicate spacecraft components or optics.

The electric fields occurring within the ion beam cause the charge-exchange ions to move approximately radially out of the ion beam. These charge-exchange ions leave the ion beam along with electrons supplied by the neutralizer. The combination of electrons and ions constituting the charge-exchange

Presented as Paper 81-0744 at the AIAA/JSASS/DGLR 15th International Electric Propulsion Conference, Las Vegas, Nev., April 21-23, 1981; submitted April 29, 1981; revision received Jan. 22, 1982.

*Assistant Professor of Physics. Member AIAA.
†Professor of Physics. Associate Fellow AIAA.
‡Associate Professor of Physics.

plasma depends on several factors, including the initial thermal energy of the ions, the distribution of ion production along the beam, the nature of the surrounding plasma, and the potentials and detailed geometry of the neighboring spacecraft surfaces.

If a monoenergetic ion beam of initial beam current J_b passes through a thickness z of a low-density neutral gas of density n_0, the number of charge-exchange ions produced per unit time is given by

$$\dot{N}_{CE} = (J_b/e)\,[1-\exp(-n_0 Q z)] \tag{1}$$

where the charge-exchange cross section is, in general, a function of the relative energy. This expression holds for a gas of low density where competing second-order processes can be neglected.

The resonance charge-exchange cross section can be considered a manifestation of the quantum mechanical probability amplitude for an electron to be localized near an ion in the neighborhood of the neutral atom to which it is originally bound. Cross sections for specific species may be obtained from the literature. A few theoretical studies[9,10] have also explored the expected behavior of the charge-exchange cross section as a function of relative energy. Functional forms obtained from these studies can be a significant aid in interpolation of energy-dependent cross-sectional data to obtain cross sections at desired energies.

Determination of the total rate of charge-exchange ion production in the beam volume must take into account both the beam current density profile of the ion thruster and the spatial distribution of neutral propellant atoms in the path of the ion beam.

For theoretical calculations a simplified ion beam current density distribution is usually chosen and axial symmetry assumed. A closed-form solution exists for only the very simplest distribution which has been used for conservative estimates of charge-exchange ion production.[8] In this case the current density is given by a Dirac delta function,

$$j_b = J_b \delta(\vec{r}). \tag{2}$$

This expression essentially places all of the beam current on the thruster axis where the neutral density follows a simple function, thus allowing a closed-form solution.

A current density profile that is more accurate for the larger, multipole thrusters is a uniform beam current density

$$j_b = J_b/\pi r_b^2 \tag{3}$$

Another profile that approximates the beam of some divergent field thrusters is a parabolic profile

$$j_b = 2J_b\,(1-r^2/r_b^2)/\pi r_b^2 \tag{4}$$

The expressions given above for the beam current density are normalized such that

$$J_b = \int_0^{2\pi}\int_0^{r_b} j_b r\,dr\,d\theta \tag{5}$$

A Gaussian profile is also used by some workers where

$$j_b = (J_b/\pi r_b^2)\,e^{-(r/r_b)^2} \tag{6}$$

subject to the normalization

$$J_b = \int_0^{2\pi}\int_0^{\infty} j_b r\,dr\,d\theta \tag{7}$$

The uniform, parabolic, and Gaussian profiles can also accommodate a defined rate of beam spreading as it propagates. The simulation described herein does not include effects from beam spreading.

Neutral gas leaving the accelerator system is taken to be in free molecular flow so that the effective neutral density at an arbitrary point, such as that shown in Fig. 1, is proportional to the subtended solid angle of the ion optics as viewed from the point (r,θ,z). Effective neutral densities were calculated numerically for an r-z matrix with a resolution of $0.1r_b$. For the near field, where about half of the charge exchange takes place, the calculated densities are given in dimensionless form in Table 1.

The calculated distribution of neutral propellant along with the beam current density profile allow a calculation of charge-exchange ion production rate per unit length as a function of distance from the ion optics.

As a first approximation, the charge-exchange production rate can be calculated in closed form if the Dirac delta function is used for the ion beam profile. The neutral density along the beam axis is given by

$$n_0(z) = \frac{n_{0,r}}{2}\left(1-\frac{z}{\sqrt{z^2+r_b^2}}\right) \tag{8}$$

where $n_{0,r}$ is defined as the density that would provide the correct loss rate of neutral propellant through an opening with the same area as the beam.

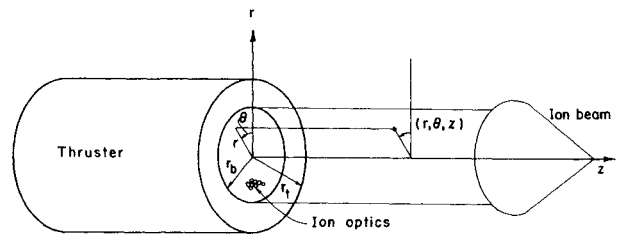

Fig. 1 Coordinate system for thruster and ion beam geometry.

Table 1 Density of neutral propellant efflux, $n_0(r,z)/n_{0,r}$

r/r_b	z/r_b 0.1	0.2	0.3	0.4	0.5	0.6	0.7	0.8	0.9	1.0
0.0	4.25×10^{-1}	4.03×10^{-1}	3.57×10^{-1}	3.15×10^{-1}	2.43×10^{-1}	2.43×10^{-1}	2.14×10^{-1}	1.88×10^{-1}	1.66×10^{-1}	1.47×10^{-1}
0.1	4.51	4.02	3.56	3.14	2.76	2.42	2.13	1.87	1.65	1.46
0.2	4.49	4.00	3.53	3.11	2.73	2.39	2.10	1.85	1.63	1.44
0.3	4.47	3.96	3.48	3.05	2.67	2.34	2.05	1.80	1.59	1.41
0.4	4.43	3.90	3.40	2.97	2.59	2.26	1.98	1.74	1.54	1.36
0.5	4.38	3.81	3.29	2.85	2.47	2.15	1.89	1.66	1.47	1.31
0.6	4.31	3.68	3.14	2.69	2.33	2.02	1.77	1.57	1.39	1.24
0.7	4.18	3.47	2.92	2.48	2.14	1.87	1.64	1.45	1.30	1.16
0.8	3.94	3.15	2.61	2.21	1.92	1.69	1.49	1.33	1.19	1.08
0.9	3.41	2.64	2.20	1.90	1.67	1.49	1.33	1.20	1.09	9.86×10^{-2}
1.0	2.15	1.91	1.72	1.55	1.41	1.28	1.67	1.17	9.75×10^{-2}	8.94

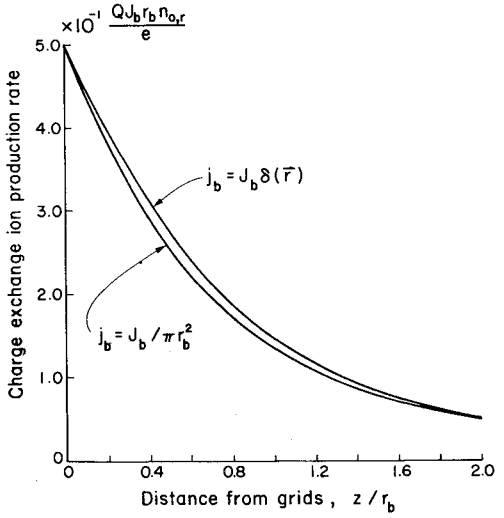

Fig. 2 Charge-exchange ion production rates for the extremes of possible beam current density distributions.

Table 2 Charge-exchange ion production rates for different beam current density profiles

Profile	Production rate $(J_b Q n_{0,r} r_b/2e)$
$J_b\delta(\vec{r})$	1.00
$2J_b(1-r^2/r_b^2)/\pi r_b^2$	0.97
$J_b/\pi r_b^2$	0.94

The neutral loss rate is then

$$\dot{N}_0 = r_b^2 n_{0,r}\sqrt{\frac{\pi kT_0}{2m_0}} \tag{9}$$

The charge-exchange ion production rate per unit length is thus

$$\dot{N}_{CE}(z) = J_b Q n_0(z)/e \tag{10}$$

for small total production rates. Integrating to obtain the total production rate gives

$$N_{CET} = J_b Q n_{0,r} r_b/2e \tag{11}$$

As the assumed ion beam profile becomes less peaked, progressing from a Dirac delta function through Gaussian and parabolic functions to a uniform distribution, the production rate of charge-exchange ions will diminish as more of the beam passes through the peripheral regions of lower neutral propellant density. The two extremes in production rates as a function of distance thus use a delta function and a uniform function for the beam profile. The results of these two extremes are shown in Fig. 2. Table 2 gives the calculated total charge-exchange ion production rates for these two extremes, as well as the intermediate parabolic ion beam profile. The ion beam profile is clearly not a dominant parameter for charge-exchange ion production.

The simulation developed to model the charge-exchange plasma propagation can accept an arbitrary input for the production rate as a function of distance.

Plasma Propagation

The physical description of the charge-exchange plasma has become well understood as the result of various studies that have been conducted. The electron distribution outside of the beam following the "barometric" equation

$$n_e = n_{e,\text{ref}}\exp(-qV/kT_e) \tag{12}$$

which has been experimentally verified by Ogawa et al.[11,12] for the population within the beam and by Kaufman[8] for the population in the charge-exchange plasma. The plasma potential V in Eq. (12) is defined as zero at the reference electron density $n_{e,\text{ref}}$. The electron temperature T_e in the charge-exchange plasma has been found to be about half the value found in the ion beam.[8] The value in the ion beam varies with thruster size and ranges from about 7 eV for a 5 cm thruster to 5 eV for 15 cm and 0.35 eV for 30 cm thrusters.

The experimental validity of Eq. (12) is consistent with the low-density and long mean free paths in the charge-exchange plasma. The decreasing plasma density with increasing distance from the thruster forms a potential well for the electrons, so that many transits of this region are probable before an electron escapes. The many transits permit randomization of the electron population to a single Maxwellian distribution by Coulomb collisions.

The extent of the charge-exchange plasma is large compared to the Debye shielding distance, which means that the electron density must everywhere equal the ion density. Inasmuch as the ions move only outward from the thruster, their motion is essentially collisionless and governed by the potential distribution from Eq. (12).

Because the charge-exchange ions have low initial velocities, they will be strongly affected by small electric fields within the beam. At the boundary between the ion beam plasma and the surrounding charge-exchange plasma, the outgoing ions are assumed to have established a velocity v_{CE} normal to the beam that is given by the Bohm criterion for a stable sheath[13]

$$v_{CE} = \sqrt{kT_e/m_0} \tag{13}$$

This is also the ion acoustic velocity. The dividing line between the ion plasma and the surrounding charge-exchange plasma is not a sharp one. An experimental distinction between the two regions can be made, however, on the basis of relative plasma densities and electron temperatures.[6]

Beginning at the boundary of the beam with a velocity equal to the Bohm velocity, the charge-exchange ions are assumed to propagate in the region surrounding the beam in the manner that is self-consistent with the local electric fields and plasma densities in that region.

Closed-Form Solution for Simplified Conditions

A theoretical closed-form solution is valuable for verification of the computer code developed to model the charge-exchange plasma propagation in the vicinity of an operating ion thruster. An analytical solution is developed herein for that purpose.

A cylindrical ion beam is assumed with a length very much greater than r_b, the beam radius. The current density representing positive charge-exchange ion production in the beam is assumed to be uniform along the beam.

In the region exterior to the beam, three basic physical conditions are assumed to hold for the ion population and/or the plasma as a whole. The first is continuity of ion current represented by

$$\vec{\nabla}\cdot j = 0 \tag{14}$$

where j is the ion current density. The barometric equation is also used to relate plasma density to local potential V

$$n_0 = n_{0,\text{ref}}\exp(e(V-V_0)/kT_e) \tag{15}$$

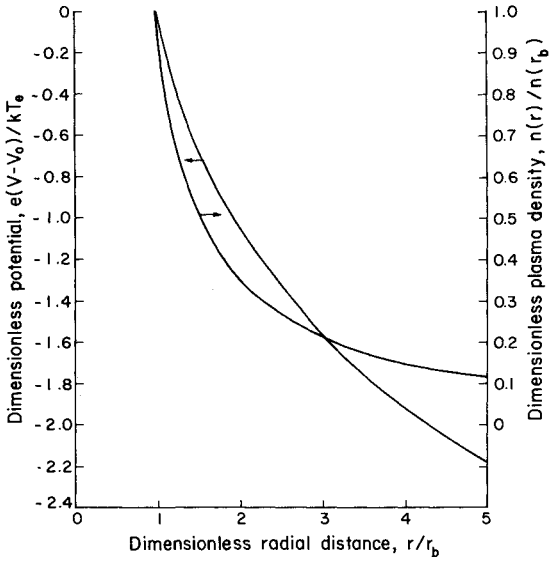

Fig. 3 Analytic solution for plasma density and plasma potential.

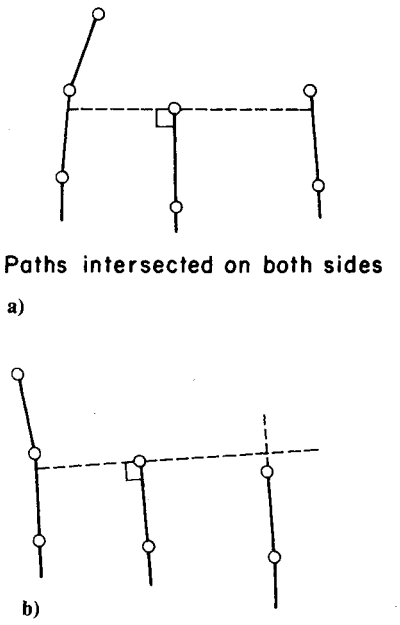

Fig. 4 Geometry for evaluation of local plasma densities between paths.

where V_0 is the potential at the reference density $n_{0,\text{ref}}$ and T_e is the electron temperature in the region exterior to the beam. Finally, energy conservation for singly charged ions is represented by

$$|\vec{v}| = (v_{CE}^2 - 2e(V-V_0)/m_0)^{1/2} \tag{16}$$

where $\vec{v}$ is the ion velocity and m_0 is the ion mass. As a boundary condition at the beam edge, ions are assumed to have acquired the Bohm velocity

$$v_{CE} = (kT_{eb}/m_0)^{1/2} \tag{17}$$

where T_{eb} is the electron temperature in the beam.

The ion current density is related to the streaming velocity by

$$\vec{j} = ne\vec{v} \tag{18}$$

For the assumed symmetry, the velocity is radial and is

$$\vec{v} = v(r)\hat{r} \tag{19}$$

where $\hat{r}$ is a unit vector in the radial direction. In cylindrical coordinates, Eq. (14) can be written with the substitution of Eq. (18) as

$$\frac{1}{r}n(r)v(r) + n(r)\frac{\partial v(r)}{\partial V}\frac{\partial V(r)}{\partial r} + v(r)\frac{\partial n(r)}{\partial V}\frac{\partial V(r)}{\partial r} = 0 \tag{20}$$

which can be solved for $V(r)$ by eliminating $n(r)$ and $v(r)$ using Eqs. (15) and (16). The solution can then be written as

$$(1 - e(V-V_0)/kT_e)e^{(-e(V-V_0)/kT_e)} = r/r_b \tag{21}$$

The density and velocity can be calculated using Eq. (21) along with Eq. (15) or (16).

The solution in terms of potential and density is displayed in dimensionless form in Fig. 3. The results for velocity will be shown to compare favorably with the output of the computer model.

Simulation Approach

A digital computer code designated PLASIM was written to simulate the propagation of the charge-exchange ions in the plasma surrounding the beam.

The approach used in this study was to assume a cylindrical, axially symmetrical ion beam with the charge-exchange ions leaving the beam with a uniform velocity in the radial direction. The current density of these charge-exchange ions at the cylindrical beam boundary is a function of the distance downstream from the thruster. The total charge-exchange current is divided equally into the total number of trajectories, with this total number specified as an input parameter. Approximately 50% of the charge-exchange ions are generated within one beam radius downstream of the thruster, so about half of the specified trajectories will initially start in this region.

A trajectory is represented as the path of a single ion in which acceleration is produced by electric fields in the plasma, which in turn are produced by gradients of the plasma density, as indicated by Eq. (12). Density gradients are used in two separate calculations. A gradient along the path serves to vary the ion velocity in that direction, while the density ratio normal to the path direction modifies the direction of the path.

In the simulation, the ion path is represented with a stepwise progression away from the beam. From a physical viewpoint, the ions are moving at or above acoustic velocity, so disturbances should not propagate in the upstream direction. Also, the extent of the plasma is very large compared to the Debye shielding distance, hence the potentials at the flow boundaries should not extend into the bulk of the plasma.

Distances to neighboring paths are used to determine densities and density ratios. The coordinates are defined in the overall configuration sketch of Fig. 1. As indicated in Fig. 4, a normal to the path being incremented is extended in both directions. This normal is used to calculate the distances to neighboring paths, on the right and left of the path being incremented. In this report, right and left are defined in terms of relationships upon leaving the ion beam with the viewing direction in the direction of charge-exchange ion motion. If the neighboring path was not intersected by a normal, as in Fig. 4b, then the neighboring path is extended linearly from the last interval. The density is inversely proportional to both the distance between neighboring paths and the radial

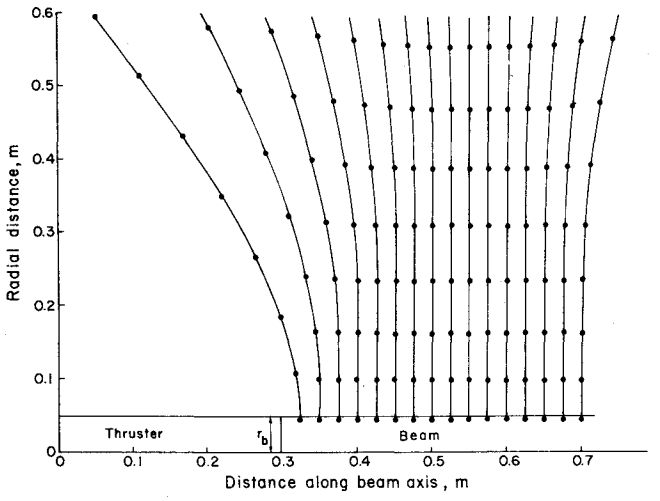

Fig. 5 Solution for uniform distribution of charge-exchange production (electron temperature 5.0 eV in ion beam and 2.5 eV in charge-exchange plasma).

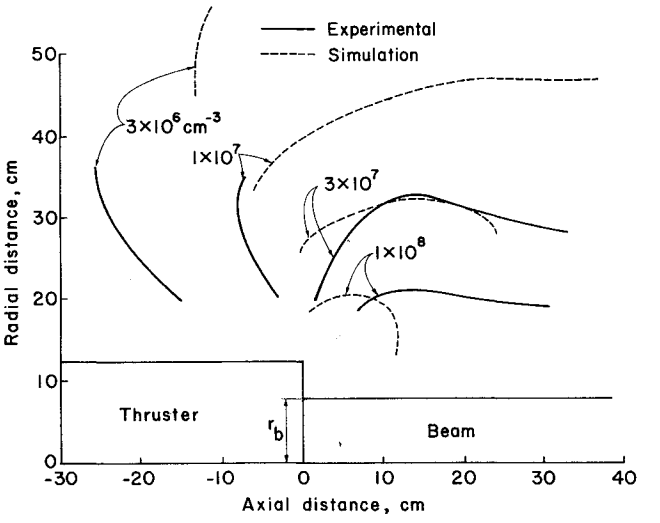

Fig. 7 Map of plasma density for 15 cm thruster with a beam current of 0.63 A and a propellant utilization of 0.85.

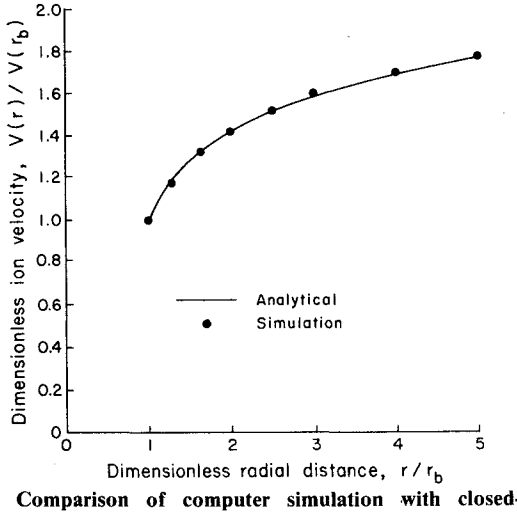

Fig. 6 Comparison of computer simulation with closed-form solution.

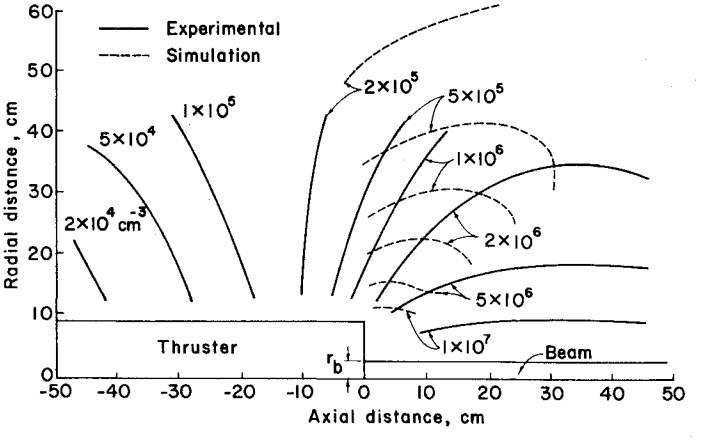

Fig. 8 Map of plasma density for 5 cm thruster with a beam current of 0.05 A and a propellant utilization of 0.71.

distance. The latter relationship is due to the axial symmetry and the use of only one trajectory for each axial location. The density on the left is thus given by

$$n_L = C/\Delta d_L r v \tag{22}$$

where C is a constant depending on operating conditions and the number of trajectories specified, and Δd_L the distance between the path being incremented and the path on the left. The density on the right is identified in a similar manner, except that n_R and Δd_R are used. The two densities can then be expressed as a ratio and used with Eq. (12) to determine a potential difference normal to the path being incremented, ΔV. Note that the constant C cancels when the density ratio is calculated. The force normal to the path direction is then

$$F_\perp = -q\Delta V_\perp / \Delta d_m \tag{23}$$

where Δd_m is the average of Δd_L and Δd_R. This force can also be defined as

$$F_\perp = m_0 \Delta v_\perp / \Delta t \tag{24}$$

with Δv the velocity component generated normal to the path direction and Δt the size of the time interval used in the iteration. Equating these two force expressions,

$$\Delta v_\perp = -q\Delta V_\perp \Delta t / m_0 \Delta d_m \tag{25}$$

This velocity change normal to the path direction is used to calculate an angular direction change. Because this velocity change is normal to the path direction, it has no effect on the magnitude of the ion velocity, only its direction.

The velocity change in the direction of ion motion is calculated using the average of the two densities (right and left). This density is compared with the same average density for the previous iteration. The ratio of average densities, with Eq. (12), yields the potential difference in the direction of motion. In a manner similar to the derivation of Eqs. (23-25), with Δd replaced by the distance $v\Delta t$,

$$\Delta v_\parallel = -q\Delta V_\parallel / m_0 v \tag{26}$$

The calculation routine advances the trajectories from left to right, starting from the thruster. If an intersection is found both to the left and right, another iteration is made. This allows paths that have less acceleration to keep in step with other paths further along, and limits the amount of extrapolation needed.

It was necessary to consider several special cases in the execution of the velocity algorithm. One was the case indicated in Fig. 4b and mentioned briefly in the discussion of density calculation. In this case the approximation made is to take the distance between the end point of the path being incremented and the linear extrapolation of the missed neighboring path.

Another case involves the furthest right and left trajectories that have not been intercepted by a boundary. Without special treatment, this case would result in an undefined density on one side of the path because the normal will intercept a boundary before it intercepts another path. The boundary is treated as another path with one exception. If at any time a path would be repelled by the boundary, the direction is left unchanged. This approximates a plasma sheath which would be present at such a boundary. In general, both the distance between trajectories and the distance from a trajectory to a boundary will be much larger than the Debye distance. The accuracy of the simulation should therefore be considered questionable at any location where the distance between trajectories approaches the distance to a boundary. A better approximation in such a location would be obtained by extrapolating from deeper within the charge-exchange plasma. It would also be possible to use more trajectories, so that the space between them would be reduced.

In practice the simulation models the ion trajectories beginning at the ion optics and extending along the beam until 95% of the total charge-exchange ion production is accounted for.

Verification

Two studies, one theoretical and one experimental, are used for the verification of the computer code. The theoretical solution is for an infinitely long cylindrical beam with a uniform production of charge-exchange ions along the beam. Because variation was assumed in only the radial direction, an analytical solution was obtainable in a straightforward manner.

A computer solution was obtained using a uniform production of charge-exchange ions along the beam and is shown in Fig. 5. The circles indicate every tenth time interval. The radial velocity obtained with the computer solution is shown in Fig. 6, together with the analytical velocity solution. The computer simulation is seen to be in excellent agreement with the analytic solution over the radius range investigated.

An experimental survey of plasma density[6] for a 15 cm source is shown in Fig. 7. The operating conditions used for Fig. 7 were duplicated in a computer simulation and the equidensity contours are shown as dashed lines. Similar results and comparison are also shown for a 5 cm source in Fig. 8. The ion trajectories associated with these equidensity contours are in good agreement with the trajectory angles measured by Carruth and Brady.[14]

Limitations

The major factor in the accuracy of simulation obtained is the number of ion paths used. At the low end of the practical range in this number, the crossing of paths will be observed. These crossings result from plasma properties changing so rapidly that the error in a path location will exceed the local path spacing. The procedure used for calculating the potential differences associated with each time interval depends on a "laminar" path structure. That is, no intersection of paths. The existence of any crossed paths therefore invalidates any local calculations of gradients, etc.

Conclusions

A digital computer simulation, PLASIM,[15] has been written and tested for modeling the propagation of charge-exchange ions outward from the beam of an ion thruster. This simulation assumes Bohm velocity for the ion leaving the beam, an isothermal charge exchange plasma, and laminar ion flow. The simulation agrees within 8% of an analytical solution based on these same assumptions. The simulation agrees in approximate magnitude with experimental measurements and is in good qualitative agreement with isodensity contour shapes and ion trajectory angles.

Acknowledgment

This work was supported by the Jet Propulsion Laboratory, Contract 955322.

References

[1] Knauer, W., Bayless, J.R., Todd, G.T., and Ward, J.W., NASA CR-72675, May 1970.

[2] Staggs, J.F., Gula, W.P., and Kerslake, W.R., *Journal of Spacecraft and Rockets,* Vol. 5, 1968, pp. 159-164.

[3] Worlock, R., Trump, G., Sellen, J.M., Jr., and Kemp, R.F., AIAA Paper 73-1101, 1973.

[4] Komatsu, G.K., Cole, R.K., Hoffmaster, D.K., and Sellen, J.M., Jr., AIAA Paper 75-428, 1975.

[5] Kaufman, H.R., NASA CR-134844, June 1975.

[6] Kaufman, H.R., NASA CR-135099, Oct. 1976.

[7] Kaufman, H.R., NASA CR-135318, Dec. 1977.

[8] Kaufman H.R. and Isaacson, G.C., AIAA Paper 76-1051, 1976.

[9] Iovitsu, I.P. and Ionescu-Pallas, N., *Soviet Physics-Technical Physics*, Vol. 4, 1960, pp. 781-791.

[10] Rapp, D. and Francis, W.E., *Journal of Chemical Physics,* Vol. 37, 1965, pp. 2631-2645.

[11] Ogawa, H.S., Cole, R.K., and Sellen, J.M., Jr., AIAA Paper 69-263, 1969.

[12] Ogawa, H.S., Cole, R.K., and Sellen J.M., Jr., AIAA Paper 70-1142, 1970.

[13] Bohm, D., *The Characteristics of Electrical Discharges in Magnetic Fields*, edited by A. Guthrie and R.K. Wakerling, McGraw-Hill Book Co., New York, 1949, pp. 77-86.

[14] Carruth, M.R. and Brady, M.E., AIAA Paper 80-1388, 1980.

[15] Robinson, R.S. and Kaufman, H.R., JPL Rept. 955322, 1980.